Interleukin-31 promotes pathogenic mechanisms underlying skin and lung fibrosis in scleroderma

Bodoor Yaseen[1*], Henry Lopez[1,2*], Zeinab Taki[1], Sarah Zafar[1], Henrique Rosario[1], Bahja Ahmed Abdi[1], Shivanee Vigneswaran[1], Fiona Xing[1], Nikita Arumalla[1], Simon Black[1], Sara Ahmad[1], Kimti Kumar[1], Rabia Gul[1], Laura Scolamiero[1], Sian Morris[1], Alex Bowman[3], Anna Stainer[3], Alexandra Rice[3], Carmel Stock[3], Elisabetta Renzoni[3], Christopher P Denton[1], Cristina Venturini[4], Max Brown[5], Steven O'Reilly[5], Richard Stratton[1]

[1]Centre for Rheumatology and Connective Tissue Diseases, Royal Free Hospital Campus, University College London Medical School, Rowland Hill Street, London, NW3 2QG, UK. [2]MuriGenics, Inc., 941 Railroad Avenue, Vallejo, CA, 94592, USA. [3]Department of Respiratory Medicine, Imperial College London, Royal Brompton Campus, Sydney Street, London SW3 6NP, UK. [4]Pathogen Genomics Unit, UCL, London, WC1E 6BT, UK. [5]Department of Health and Life Sciences, Northumbria University, Newcastle Upon Tyne, UK. *Contributed equally. Correspondence and requests for materials should be addressed to RS (r.stratton@ucl.ac.uk), Centre for Rheumatology and Connective Tissue Diseases, Royal Free Hospital Campus, University College London Medical School, Rowland Hill Street, London, NW3 2QG, UK.

Conflict of interest statement

The authors have declared that no conflict of interest exists.

Keywords

Fibrosis, IL-31, systemic sclerosis

Key messages

- IL-31 is a four helix bundle cytokine of the IL-6 family, secreted by Th2 cells.
- Plasma IL-31 levels are elevated in a subset of SSc patients.
- IL-31 is pro-fibrotic, activating fibroblasts in tissue culture, and inducing skin and lung fibrosis in mice.

Abstract

Objectives Cytokines released by infiltrating T cells may promote mechanisms leading to fibrosis in scleroderma. The aim of this study was to investigate the role of the Th2 cytokine IL-31, and its receptor IL-31RA, in scleroderma skin and lung fibrosis.

Methods IL-31 was measured by ELISA of plasma, and by immunochemistry of fibrotic skin and lung tissue of scleroderma patients. The receptor, IL-31RA, was assayed by qPCR of tissue resident cells. Next generation sequencing (NGS) was used to profile the responses of normal skin fibroblasts to IL-31. In wild-type Balb/c mice, IL-31 was administered by subcutaneous mini pump, with or without additional TGFβ, and the fibrotic reaction measured by histology and ELISA of plasma.

Results IL-31 was present at high levels in plasma and fibrotic skin and lung lesions in a subset of scleroderma patients, and the receptor overexpressed by downstream cells relevant to the disease process, including skin and lung fibroblasts, through loss of epigenetic regulation by miR326. In skin fibroblasts, IL-31 induced NGS profiles associated with cellular growth and proliferation, anaerobic metabolism and mineralisation, and negatively associated with angiogenesis and vascular repair, as well as promoting phenotype changes including migration and collagen protein release via pSTAT3, resembling the activation state in the disease. In mice, IL-31 induced skin and lung fibrosis. No synergy was seen with TGFβ, which supressed IL-31RA.

Conclusions. IL-31/IL-31RA is confirmed as a candidate pro-fibrotic pathway, which may contribute to skin and lung fibrosis in a subset of scleroderma patients.

Introduction

Scleroderma (systemic sclerosis, SSc) is a heterogeneous disease in which dysregulation of the immune system is linked to microvascular damage and fibrosis(1). This triad can manifest in multiple organs, including the skin, lungs, kidneys, heart and gastrointestinal tract. Lung involvement is a major clinical feature linked to long-term outcomes and reduced survival in SSc(2). Although the definite etiology that evokes the consecutive pathogenic response is not completely understood, recent epigenetic and genome wide

association studies (GWAS) have reported several genetic variants in immunoregulatory genes associated with susceptibility to the disease(3-5).

The underlying mechanisms that link SSc-associated genetic variants with the initiation or progression of the disease are yet to be fully evaluated. However, many studies have investigated the negative impact of the cross-talk between immune cells, inflammatory cells and mesenchymal cells during SSc pathogenesis. The initial examination of cellular infiltrates in skin and lung biopsies isolated from SSc disclosed an involvement of T cells and macrophages in the onset of early disease(6, 7). Further studies have confirmed elevated levels of cytokines in SSc and have implicated T-cell derived factors in the cross-talk with fibroblasts(8-10). Aligned with an autoimmune process, placebo controlled studies have indicated benefit from immunosuppressive drugs as well as autologous haematopoietic stem cell transplantation(11-13) .

Interleukin 31 (IL-31) was identified by Dillon in 2004 as a 4 alpha-helix IL-6 family cytokine synthesised by activated Th2 cells(14). IL-31 acts via a heterodimeric receptor comprising IL-31RA and oncostatin M, expressed by multiple cell types, and signaling via PI3K, ERK and JAK/STAT pathways(15). IL-31 has a role in pruritic skin conditions such as atopic dermatitis and T cell lymphoma, where elevated plasma levels may correlate with itch severity(16, 17). Moreover, nemolizumab, a monoclonal anti-IL31RA, reduced itch severity and corticosteroid use in patients with atopic dermatitis(18). However, the precise role of the IL-31/IL-31RA axis in promoting skin pathology is not fully understood. Aside from provoking itch behavior, this pathway induces chemokines, enhances recruitment and activation of inflammatory cells, and may cause tissue remodeling(19-21). Since Th2 cells have been implicated in initiating fibrosis, and because severe and resistant pruritus affects 40-60% of SSc patients(22, 23) the IL-31/IL31RA axis may be of relevance to this disease. Here we investigate IL-31/IL31RA as a candidate pathway in SSc skin and lung fibrosis.

Materials and Methods

Patients studied and ethical approval. Studies were performed in concordance with the agreement of Helsinki. Clinical material used in this study, such as skin biopsies and blood samples, were collected by clinical research fellows from SSc patients recruited via the Royal Free Hospital, who met internationally agreed criteria for diagnosis(24). Ethical Committee approval for this study was obtained from the NHS Health Research Authority,

NRES Committee London, Hampstead, Research Ethics Committee London Centre, reference number 6398. Clinical characteristics of the patients studied by plasma analysis are shown in the Supplementary information, "Patients included" Tables S1 and S2.

Assays for interleukin-31

All blood samples were taken into EDTA tubes and stored as aliquots of plasma at -80°C, prior to assay by ELISA. The first group of patients and controls were studied prospectively (Table S1) and plasma IL-31 was assayed by ELISA (R&D systems, #DY2824). In a replicate group (Table S2), patients were identified via a database, and stored plasma samples were assayed by a second ELISA (Human IL-31 ELISA MAX™ Deluxe #445704, Biolegend).

Cell culture. Primary human dermal fibroblasts were established from explants of the forearm skin punch biopsies (4mm) from healthy controls and from the involved skin of SSc patients (both n=4 cell lines). Primary adult pulmonary fibroblasts were cultured from control tissue samples (unaffected lung peripheral to resected cancer) and from surgical lung biopsy samples of patients with SSc (both n=4 cell lines). Dermal and lung fibroblasts were cultured by explant of minced tissue, as described previously (25) and treated as follows: TGFβ (4 ng/ml, #240-B, R&D system), IL-31 (1-100 ng/ml, R&D system), 1 μM 5-azacytidine (5-aza, #A1287 Sigma).

Quantitative PCR. SSc and healthy control fibroblast cell lines (both n=4), were lysed for RNA extraction and purification by Qiagen RNeasy Plus Mini Kit's (# 74134). Qiagen Quantifast SYBR green kit was used to prepare the qPCR reaction and Rotogene6000 series software 1.7 was used to analyse the results. The TBP gene was used as the housekeeping gene to normalize the studied genes' expression. Forward and reverse primers used for each gene are listed in (Table 1).

Gene	Forward Primer	Reverse Primer
TBP	5'- AGTGACCCAGCATCACTGTTT -3'	5'-GGCAAACCAGAAACCCTTGC -3'
IL31RA	5'- GATGTGCGGTCAAGGAGTCA -3'	5'- GCCACATGGAGCTTCTTCCT -3'
CTGF	5'-GACCTGGAAGAGAACATTAAGAAGG -3'	5'- TGAGTATGTCTTCATGCTGGTG -3'
COL1A2	5'- TGCTTGCAGTAACCTTATGCCTA -3'	5'- CAGCAAAGTTCCCACCGAGA -3'

Table 1. Forward and reverse primers; TBP, TATA box binding protein, IL-31RA, interleukin 31 receptor alpha, CTGF, connective tissue growth factor.

Western blotting. Fibroblast cell lines were lysed using RIPA buffer containing phosphatase inhibitors. Total protein concentration in the lysates was determined using the Bicinchoninic Assay Kit (Life technology). Protein extracts were separated by SDS-

PAGE, and then transferred to a nitrocellulose blot membrane, then probed with antibodies as follows; CTGF (1:500/1:1000) #sc14939, Santa Cruz), Collagen I (1:3000, #ab34710, Abcam), AKT (1:1000, #9272, Cell Signalling Technology), pAkt (1:1000, #9271, Cell Signalling Technology), STAT3 (1:1000, #9145, Cell Signalling Technology), pSTAT3 (1:2000, #9145s, Cell Signalling Technology) and GAPDH (1:50,000/1:10,000, #ab8245, abcam) overnight at 4°C. Species specific secondaries were used followed by development with the ECL western blotting detection system (GE Healthcare Life Sciences).

Immunostaining of skin and lung biopsies. 4mm punch biopsies were removed from the anterior forearm from healthy controls and SSc patients (both n=6). Lung tissue was obtained from surgical biopsies of SSc involved fibrotic lung and from healthy tissue adjacent to cancer lung biopsies (both n=10). The biopsies were frozen in OCT and sectioned. Rabbit polyclonal anti-human IL-31 primary antibody (1:50, #PA5-26394, Invitrogen) and anti-rabbit secondary antibody labelled with HRP were used for immunostaining.

In the lung studies, cellular type was identified morphologically by an experience lung pathologist (AR). A semiquantitative 4-tiered scoring system of absent, mild, moderate and marked (0-3) was used to evaluate the number of positively stained cells for each cell type, including alveolar macrophages, inflammatory cells, alveolar epithelial cells, type 2 pneumocytes and bronchial epithelial cells.

Next generation sequencing. Healthy control dermal fibroblasts (n=4 replicate skin fibroblast cell lines) were cultured in 24 well plates until they reached 100% confluence, transferred to low serum overnight and then treated for 16 hours with media only or IL-31(50ng/ml) suspended in 0.2% serum with DMEM. RNA extraction was by Qiagen RNeasy extraction kit, assayed by UCL Genomics Centre using Illumina TrueSeq standards library with 15 million reads per sample. High Sensitivity Tapestation kit and 43 paired end sequencing were used as the quality control of the samples.

Transcriptome analysis. Paired end reads were mapped to the Ensembl human transcriptome reference sequence (latest version available during analysis: GRCh38[47]). Mapping and generation of read counts per transcript were done using Kallisto (doi:10.1038/nbt.3519) based on the novel idea of pseudoalignment. R/Bioconductor package tximport was used to import the mapped counts data and summarise the transcripts-level data into gene level as described in this paper. Further analyses were run

using DESeq2 package. Normalisation and differential analysis were carried out according to the DESeq2 model by use of negative binomial generalized linear model. The estimates of dispersion and logarithmic fold changes incorporate data-driven prior distributions. Using this method, the results for the two experimental conditions were compared, and shown as a results with $\log_2$ fold changes, Wald test p values and adjusted p values (according to false discovery rate). Mapped reads for each sample ranged between 12 and 21 million. Principal component analysis was used as a quality control assessment.

Functional classification of differentially expressed genes was performed using Ingenuity Pathway analysis (IPA, https://www.qiagenbioinformatics.com/). The "core analysis" function was used to interpret the data in the context of biological processes, pathways and networks. Significance of the biofunctions and the canonical pathways were tested by the Fisher Exact test p-value. Networks were constructed using the focus molecules from the dataset obtained from the NGS and the database used by the IPA software, Knowledge Base, used to fill areas lacking connectivity with predicted non-focus molecules. Countplots of differentially expressed genes were produced using Graphpad prism 7.0.

Migration assay. Migration was studied using a standard scratch migration assay(26), during which cells were treated with 0.2% serum(negative control), 10% serum (positive control), 50ng/ml of IL-31 in 0.2% serum, or IL-31 (50ng/ml) plus Wortmannin (100 nM, PI3K inhibitor) or U0126 10µM (ERK pathway inhibitor), in SSc and control dermal fibroblasts (both n=4 dermal fibroblast cell lines), and migration quantified by Axioscope imaging. Scratch area was measured using NIH ImageJ software.

Mouse model. 6-8-week-old male Balb/c mice (Charles River Laboratories, CA) were used to study the *in vivo* pro-fibrotic effect of IL-31. A mini ALZA osmotic pump implanted in the skin pumped one of the following treatments continuously over 14 days: Saline control (n=7 mice), 200 ng of IL-31 (#210-31-10, Peprotech) per day (n=6), 800 ng TGFβ per day (cyt-8585b, Prosec)(n=7) or IL-31 with TGFβ(N=6). On day 14 the mice were anaesthetized and the pump was removed. On day 21, mice were euthanised and skin sections adjacent to the mini-pump, as well as the lungs, were obtained and stained by picrosirius red (PSR) and Masson's Trichrome. Plasma samples from day 21 were assayed for PDGF-BB (#MBB00, PDGF-BB ELISA, R&D), TGFβ 1 (#MB100B, TGFB1 ELISA, R&D) and IL-6 (#M6000B, IL-6 ELISA, R&D).

The same protocol was followed to obtain and study lung tissue at a later timepoint with n=5-6 mice per treatment group and euthanasia performed on day 42. Ashcroft scoring was used to quantify central and peripheral pulmonary fibrosis(27).

Statistical analysis. Plasma and BF levels of IL-31 were compared by non-parametric analysis using Mann Whitney U-test. In tissue culture and mouse biology experiments, ANOVA followed by Tukey's post hoc test, was used to compare multiple groups. Correlation between level of IL-31 and clinical parameters were assessed using Pearson correlation test. P values ≤ 0.05 were considered significant. GraphPad prism 8.1.1 was used to carry out these analyses.

Results

Gene database analysis of IL-31 and IL-31 receptor expression by cell type. Genevestigator analysis indicated that IL-31 expression was specific to Th2 cells, whereas the receptors IL31RA and OSMR were expressed by multiple tissue resident cell types, including dermal fibroblasts, pulmonary fibroblasts, fat-derived mesenchymal stem cells (MSCs), monocyte-derived macrophages, and vascular smooth muscle cells (Fig. 1a). These data support a model in which IL-31 is synthesised predominantly by Th2 cells, but potentially acting on multiple tissue resident cells relevant to fibrosis.

Levels of IL-31 in plasma, blister fluid and fibrotic tissue of SSc patients. Initially levels of IL-31 were measured in plasma samples collected prospectively from 27 healthy controls (HC) and 62 SSc patients, revealing elevated IL-31 in SSc (HC: 0.7-793, median 55; SSc: 0.7-17764 median 194 (pg/ml), p<0.039, Mann-Whitney U-test); (Fig.1b). For validation, a further analysis of stored plasma samples was performed using plasma from 49 HC and 100 SSc patients (50 limited cutaneous and 50 diffuse cutaneous subset), confirming elevated plasma IL-31 in SSc (HC: 0.7-1056, median 8, SSc 0.7-36564, median 117 pg/ml, p<0.0001 Mann-Whitney U-test)(Fig. 1c). However, plasma IL-31 levels did not correlate with disease subset, modified Rodnan Skin Score, disease duration or ESR (data not shown). Of interest, plasma IL-31 was below the limit of detection of the assay in 9 of 27 HC versus 11 out of 62 SSc in the first assay (Chi square test NS), and in 22 out of 49 HC versus 11 out of 100 SSc in the second assay (Chi square test $p<2.8\times10^{-6}$). Dichotomous presence or absence of IL-31 detection in plasma samples is a well-established finding in previous studies (16, 17, 28).

In tissue, IL-31 positive cells were identified in inflammatory infiltrates in the perivascular areas and epidermis of the involved SSc skin but not in biopsies from healthy controls (seen in 2 out of 6 SSc skin biopsies)(Fig. 1e). Histologic scoring of the 10 SSc and HC lung biopsies indicated significant elevation of IL-31 positive inflammatory cell infiltrates in SSc ($p < 0.035$, Fisher's exact test), and a trend towards increased epithelial staining in SSc ($p < 0.07$) (data shown in "Supplementary information-Lung tissue immunostaining for IL-31", and Fig. 1f,g).

Expression levels of the IL-31 receptor in SSc pathogenic cells. As assessed by qPCR of SSc and control cell lines (n=4 cell lines per group), the IL-31RA receptor was expressed at a higher level by both the dermal ($p < 0.015$, ANOVA followed by Tukey's test) and lung fibroblast ($p < 0.016$) from SSc patients when compared to controls, and to a similar level by fat derived MSCs (single pooled HC MSC culture) (Fig. 1d).

IL-31 induces differential RNA expression in skin fibroblasts. IL-31-treated healthy dermal fibroblast (n=4 normal dermal fibroblast cell lines cultured with or without IL-31 (50ng/ml)) were analysed by NGS, revealing significantly altered gene expression patterns (Figure 2A); integrin signaling pathway, fMLP in neutrophils, PI3K/AKT signaling and actin nucleation by ARP-WASP complex were all upregulated. In contrast, the canonical pathways which were deactivated, included planar cell polarity (PCP), colorectal cancer metastasis, cardiovascular associated-hypoxia signaling, Wnt signaling and others. Moreover, the IPA software was used to predict the possible biological consequences of IL-31 stimulation of fibroblasts, based on grouping the activated molecules into different functional categories (shown in Table 2). 561 molecules were reported to be expressed differentially in IL-31 treated dermal fibroblasts. Of these, 200 molecules associated with cell proliferation and growth were found to be upregulated. Other upregulated molecules were related to functions including lactic acid production, apoptosis and differentiation of fibroblasts, cell death of endothelial cells, and mineralization of connective tissue cells. Meanwhile, the suppressed molecules were involved in vasculature development, angiogenesis and vasculogenesis.

Categories	Functions	Diseases or Functions Annotation	p-Value	Z-score	Number of molecules involved/561
Carbohydrate Metabolism, Small Molecule Biochemistry	production	production of lactic acid	0.00368	-2.021	5
Cellular Growth and Proliferation	proliferation	proliferation of cells	4.5E-13	-1.589	200
Cell Morphology	mineralization	mineralization of connective tissue cells	0.000473	-1.358	5
Cell Death and Survival	apoptosis	apoptosis of fibroblast cell lines	0.000175	-1.219	23
Cell Death and Survival, Organismal Injury and Abnormalities	cell death	cell death of endothelial cells	0.00612	-0.904	11
Cellular Development, Connective Tissue Development and Function	differentiation	differentiation of fibroblast cell lines	0.00419	-0.73	12
Cell Death and Survival	apoptosis	apoptosis of fibroblasts	0.000117	-0.694	17
Cardiovascular System Development and Function, Organismal Development	angiogenesis	angiogenesis	6.71E-05	0.085	52
Cardiovascular System Development and Function	development	development of vasculature	6.12E-06	0.106	62
Cardiovascular System Development and Function, Organismal Development	vasculogenesis	vasculogenesis	0.000631	0.254	41

Table 2. Analysis of disease and functional gene expression in IL-31 treated dermal fibroblasts. This analysis predicts the affected physiological process in response to IL-31 treatment, based on gene expression and the directional changes. Upon IL-31 stimulation, 561 molecules were differentially activated. Each category shows the functional or the pathological process and the number of molecules involved in the process. P values less than <0.05 were considered significant and activated processes are indicated by negative z-scores. Functions highlighted by shading are predicted to be upregulated by IL-31, and non-shaded rows refer to downregulated functions. p values were generated by Fisher Exact test.

To put the data obtained from NGS into context, the knowledge-based feature in IPA was used to construct a hypothetical map network. The network with the highest score and significance, displayed proteins involved in cellular movement, cell-to-cell signaling and interaction, and cellular development (Fig. 2B). The second highest score was for the network responsible for functions categorized as inflammatory response, and hematological system development and function (Fig. 2C). The first network had 26 focus molecules and ERK1/2 as the central node, whereas the second network showed 16 focus molecules and IL-6 was the central node. Various candidate genes relevant to SSc were induced by IL-31, including: Interleukin-33 (*IL33*, p=0.043), C-X-C motif chemokine 5 (*CXCL5*, p=0.005) and Annexin 1 (*ANXA1*, p=0.02) (all by Wald's statistic test) (shown in Fig. 2D).

Phenotype changes induced by recombinant IL-31. Initially a dose-response was obtained by treating healthy dermal fibroblasts (n=2 cell lines studied) to increasing concentrations of IL-31 (1-100 ng/ml) in the presence or absence of the known pro-fibrotic TGFβ (4ng/ml), using collagen I protein as readout for the fibrotic response. IL-31 treatment led to induction of collagen I, which was maximal with 50 ng/ml of the recombinant protein (Fig.

3a). However, no induction of the matricellular fibrotic protein CTGF was seen in normal dermal fibroblasts (n=4 cell lines) treated with IL-31 50 ng/ml (Fig. 3B). As expected, TGFβ induced the production of both collagen I and CTGF(Fig. 3A-B). Unlike the collagen I protein, mRNA levels of type I collagen were not increased by the IL-31 treatment, indicating non-transcriptional regulation of collagen I protein synthesis (n=4 cell lines)(Fig. 3F). In replicate experiments (n=4 cell lines) normal dermal fibroblasts exhibited elevated collagen I following treatment with IL-31 (50ng/ml) (mean Western band intensity, basal 0.723, IL-31 treated 1.03 (p<0.032), TGFβ 1.06 (p<0.033), IL-31+TGFβ 0.98 (p NS)(paired T test)(Fig. 3C). SSc dermal fibroblasts demonstrated more variable and higher basal collagen I and no significant induction when stimulated by IL-31 (basal 0.87, IL-31 0.95, TGFβ 1.32, IL-31+TGFβ 1.11 (all p NS vs basal)(Fig. 3C). This pattern of high basal activity and less marked induction by pro-fibrotic stimuli is a known feature of SSc fibroblasts. No positive synergy between IL-31 and TGFβ was observed; in fact the effects of adding both agents together reduced the maximal collagen I protein response (Fig. 3C).

Furthermore, phosphorylated STAT3 bands were seen after 5 minutes of treatment with IL-31, reduced by 60 minutes, whereas pAkt was seen after 30 minutes, indicating active signalling through STAT3 and PI3K/Akt pathways (n=2 normal dermal fibroblast lines) (Fig. 3D). When dermal fibroblasts were treated with the STAT3 inhibitor SD1029, collagen I induction by both IL-31 and TGFβ was blocked, confirming the role of STAT3 signalling in the fibrotic response (n=1 dermal fibroblast lines for SSc and controls) (Fig. 3E).

Moreover, IL-31 was found to increase the migratory behaviour of HC and SSc dermal fibroblasts (both n=4), reduced when PI3K inhibitor (Wortmannin, 100nM) or MEK/ERK inhibitor (U0126, 5μM) were added (both studied at a single known inhibitory dose) (p<0.001) (Fig.3G).

Assessing the in vivo pro-fibrotic activities of recombinant IL-31. In wild type Balb/c mice, IL-31-treatment resulted in dermal thickening, and increased cross-linked dermal collagen as assayed by PSR stain, whereas TGFβ alone failed to induce comparable results, and showed no synergy when combined with IL-31(Fig. 4A,B).In lung tissue no significant fibrotic pathology or cellular infiltrate was seen on day 21 (data not shown). However, on day 42, IL-31 treatment resulted in significant fibrosis most apparent in the central lung area (Fig. 4C). Also, in IL-31 treated mice there was a non-significant trend towards elevated plasma levels of IL-6, TGFβ1 and PDGF, compared to saline receiving mice (Fig. 4D).

IL-31RA regulation See Supplementary data-"Regulation of IL-31RA".

Discussion

Whereas initial interest focused on its role as a pruritogenic factor in atopic conditions, more recent studies have indicated pro-inflammatory and tissue remodeling effects, and demonstrated increased expression levels of IL-31 in autoimmune connective tissue disorders such as SLE and dermatomyositis (29, 30). Here, in the first study of IL-31 in SSc, we show elevated levels in a subgroup of patients. Current concepts indicate that SSc is a heterogeneous disease with distinct pathogenic subgroups, emphasising the potential for complex and variable underlying disease processes(31), which in this instance may involve this Th2 cytokine in the immune-fibrotic pathology. Our findings indicate very high plasma levels of IL-31 in around 10% of patients, with levels in the ng/ml range likely to influence target cells. However, we were unable to identify a clear clinical pattern for this subgroup, which is a limitation of the study.

Furthermore, since the precise reason for the widespread tissue distribution of the IL-31RA receptor is not fully understood, we investigated and confirmed a tissue remodeling effect. Treatment with IL-31 in fact led to the differential expression of multiple genes and SSc disease-relevant pathways in dermal fibroblasts. Also, IL-31 elevated collagen I protein release via pSTAT3, a known SSc-like phenotype(32). The fibrotic activation by IL-31 did not synergise with that induced by the classical pro-fibrotic factor TGFβ, which reduced IL-31RA receptor levels. It is possible that the IL-31-induced fibroblast activation, and that induced by TGFβ, represent different phases of a disease process, which are only partially overlapping.

The receptor IL-31RA appeared increased in skin and lung fibroblasts from SSc. Persistent elevation of IL-31RA in pathogenic cells could be explained through epigenetic mechanisms, and consistent with this, we demonstrated that IL-31RA is regulated by a microRNA in healthy control cells, an effect which is reduced in SSc.

In fact, a pro-fibrotic role for IL-31was confirmed, inducing dermal and lung fibrosis in mice, and resembling certain aspects of the clinical disease such as thickening of the dermis and increased local collagen, but not leading to loss of subcutaneous fat. Furthermore, any effect on vascular health was not evaluated, as a limitation of the study.

Treating progressive skin and organ-based fibrosis in SSc remains a significant unmet need despite recent progress (33). The underlying complex pathology, the diverse involvement of inflammatory and immune cells which act upstream of signaling events in fibroblasts, and the heterogeneity from patient to patient are ongoing challenges. It is possible that in certain SSc patients IL-31 is promoting the inflammatory-fibrotic pathology seen. Targeting T cell derived cytokines such as IL-31 is achievable with current therapies, and might reduce the burden of pruritus and fibrosis in this severe disease (18).

Author Contributions

BY performed cell biology experiments with skin and lung fibroblasts, qPCR, western blotting and wrote the manuscript. HL performed mouse biology experiments. ZT performed cell biology experiments with dermal fibroblasts, carried out the migration and arranged genomic analysis. SZ collected and assayed dermal blister fluid for protein expression. CV performed next generation sequencing analysis of the data. SNA, SV, KK, RG, CD and NA provided dermal blister fluid, plasma samples and clinical database correlation. SM performed ELISA assay and, with HR, performed dermal immunohistochemistry. SB performed skin biopsy and immunohistochemistry. ER, AB, AS and AR & CS performed lung histology analysis and provided lung fibroblast cell lines. BAA performed cell biology experiments and western blots. LS performed database analysis and contributed to the writing of the manuscript. SOR and MB performed epigenetic studies involving miRNAs. RS conceived the study reviewed the manuscript and figures.
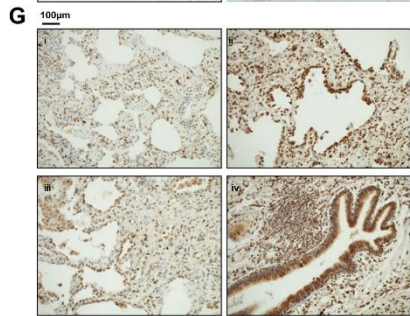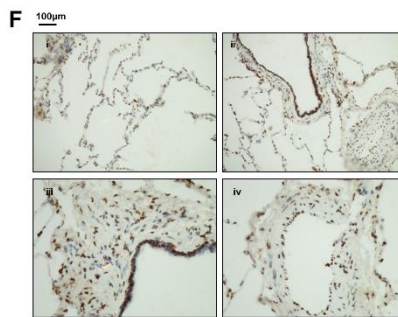
A

mRNA expression level

IL31RA

OSMR

IL31

- Bronchial epithelium cell
- Monocyte-derived macrophage
- Microvascular endothelium cell
- Macrophage
- Epidermal keratinocyte
- Dendritic cell
- Bone marrow-derived mesenchymal stem cells
- Pulmonary fibroblast
- Dermal fibroblast
- Peripheral blood CD8 activated T-cell
- Vascular smooth muscle cell
- Synovial fibroblast
- B-cell
- Fat-derived mesenchymal stem cell
- Peripheral blood CD4 naïve T-cell
- Peripheral blood CD4 activated T-cell
- Pulmonary microvessel endothelium cells
- Umbilical cord blood Th2 T-cell
- Umbilical cord blood Th1 T-cell

B Plasma IL-31

p<0.039

IL-31 (pg/ml)

HC   SSc

C Plasma IL-31

p<0.0001

IL-31 (pg/ml)

HC   SSc

D IL-31RA

Relative expression

p<0.015   p<0.016

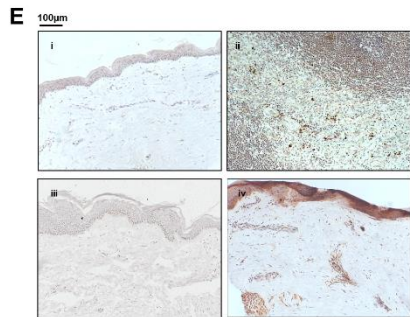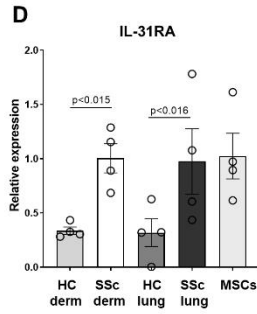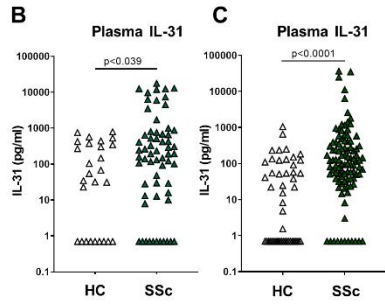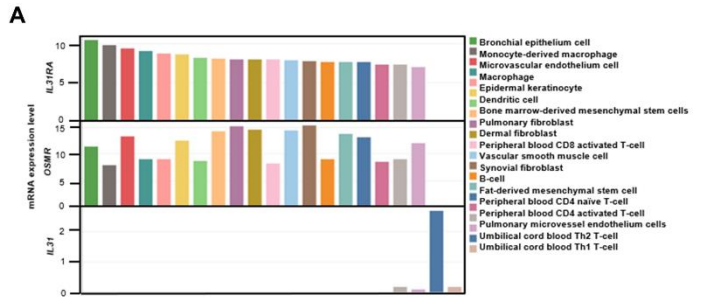HC derm   SSc derm   HC lung   SSc lung   MSCs

Fig.1 Relevance of IL-31/IL-31RA to skin and lung fibrosis in scleroderma.(**A**) Expression levels of IL31,OSMR,IL31RA by genevestigator, gene database software, showing the log2 mean gene expression. IL-31 expression appears specific to peripheral blood activated CD4+ Th2 cells, whereas the receptors IL31RA and OSMR are expressed by multiple tissue resident cells of potential relevance to fibrosis.(**B**) Plasma samples from HC and SSc patients were collected prospectively and assayed by ELISA for IL-31, showing elevated levels in SSc patients. (**C**) Further stored samples from SSc patients and controls identified via a database were assayed by ELISA, confirming the elevated plasma levels. (**D**) Potential downstream cellular targets of IL-31 were profiled for the receptor IL-31RA expression by qPCR. IL-31RA was elevated in both skin and lung fibroblasts from SSc versus healthy controls (all n=4 cell lines per group) and expressed to a similar level by adipose derived MSCs (a single pooled cell line). (**E**) Immunostaining of skin biopsies taken from the affected area of the forearm skin from SSc patients and HCs (n=6 biopsies for HC and SSc). (i) Negative control with no primary IgG, (ii) positive control with normal spleen tissue, (iii) HC with anti-IL-31, (iv) SSc involved skin with anti-IL-31, indicating positive IL-31 expressing cells in perivascular infiltrates and in the epidermis seen in 2 out of 6 patient samples and 0 of 6 control samples. (**F**) HC lung sections were examined (n=10) showing as follows; (i) alveolar tissue showed only weak expression, (ii) in bronchial tissue positive staining of bronchial epithelial cells, and (iii) in peribronchial interstitial lymphocytes and (iv) some vascular endothelial and smooth muscle cells. (**G**) However, in SS lung biopsies (n=10) variable but in some cases strong immunostaining seen in (i) interstitial lymphocytes, (p<0.035, see table S3 for histologic scoring)(ii) & (iii) type 2 pneumocytes, as well as in (iv) bronchiolar epithelium (p<0.07) and peribronchial lymphoid aggregates. P values indicate Mann-Whitney U test for B and C, and ANOVA and Tukey's test were used for D.

A

-log(p-value)

0   1   2   3   4   5   6

pathway

- PCP pathway
- Cardiac hypertrophy
- Colorectal cancer metastasis
- Hypoxia signalling in the cardiovascular system
- Integrin Signalling
- fMLP signalling in neutrophils
- PI3K/AKT signaling
- Actin nucleation by ARP/WASP complex
- Wnt/calcium pathway
- ATM signaling
- Phospholipase C signaling
- TGFβ signaling
- G-beta-gamma signaling
- CXCR4 signaling
- IL8 pathway
- Regulation of actin based motility by Rho
- PTEN signaling
- Thrombin signalling

■ pathways activated by control media and deactivated by IL31
■ pathways deactivated by control media and activated by IL31
transparency of the bars indicate Z-score of the pathway.

B

C

D

IL-33

Expression

p=0.043

Media   IL-31

CXCL5

Expression

p=0.05

Media   IL-31

ANXA1

Expression

p=0.02

Media   IL-31

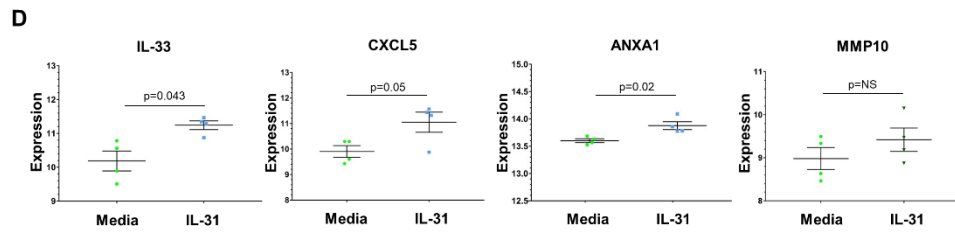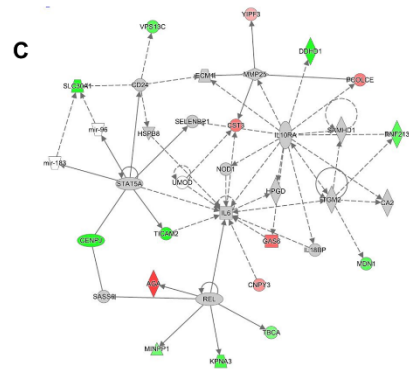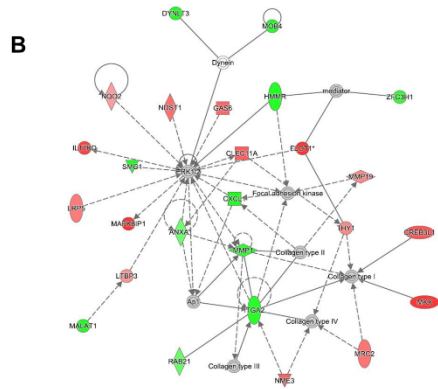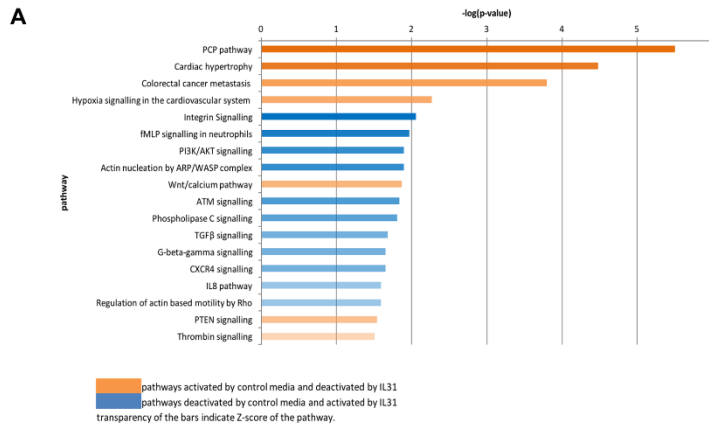MMP10

Expression

p=NS

Media   IL-31

Fig.2 Next generation sequence analysis of dermal fibroblast after treatment with IL-31 (A) IPA pathway analysis of canonical pathways activated and deactivated in fibroblasts by IL-31 treatment. Healthy dermal fibroblasts were treated with either media containing 0.2% serum or media containing 0.2% serum plus IL31 (50ng/ml). Bars in orange indicate pathways deactivated by IL-31 and those in blue, pathways activated by IL-31. The barplot orders the most activated/deactivated pathways. The X-axis measures the significance of the activation/deactivation (p values calculated by Fisher exact test). Transparency of the bars illustrates the z-score calculated, darker bars have higher z-scores. **(B)** Networks involved in IL31 treatment of dermal fibroblasts were predicted by IPA. The network most strongly correlated with IL-31 treatment identiifed genes involved in cellular movement and centered on ERK1/2, with a score of 33 with 26 focus molecules. **(C)** A second network identified genes involved in the inflammatory response, centered on IL-6, and with a score of 16, with 16 focus molecules. Nodes in green are activated by IL31. Red nodes are of genes deactivated by IL31. Darkness of the colour illustrates Z-score. Darker colours have more significant directionalities. Grey nodes are filled in by the Ingenuity Knowledge Base. P values were generated by Fisher Exact test. **(D)** Examples of candidate factors relevant to SSc and induced in healthy dermal fibroblast after IL-31 treatment (Y axis values log2 RNA seq). IL-33, interleukin-33; ANXA1,annexin 1;CXCL5, C-X-C motif chemokine5;MMP10,matrix metallopeptidase 10, P values were determined with Wald's statistic test.

A

Collagen I
115kDa

GAPDH
37kDa

IL-31 0 1 1 2.5 2.5 5 5 10 10 50 100 0 (ng/ml)
TGFβ   +   +   +   +   +   +

B

CTGF
38 kDa

GAPDH
37kDa

IL-31   50   50   50   50 (ng/ml)
TGFβ   +   +   +   +
          HC1   HC2   HC3   HC4

C

HC1   HC2
Collagen I
115 kDa

GAPDH
37kDa

HC3   HC4
Collagen I
115 kDa

GAPDH
37kDa

Ctrl IL-31 TGFβ IL-31   Ctrl IL-31 TGFβ IL-31
                   +TGFβ   +TGFβ

SSc1   SSc2
Collagen I
115 kDa

GAPDH
37kDa

SSc3   SSc4
Collagen I
115 kDa

GAPDH
37kDa

Ctrl IL-31 TGFβ IL-31   Ctrl IL-31 TGFβ IL-31
                   +TGFβ   +TGFβ

Collagen I

p<0.033
p<0.032

Western band intensity

1.5

1.0

0.5

0.0

Ctrl IL-31 TGFβ IL-31+TGFβ Ctrl IL-31 TGFβ IL-31+TGFβ

D

HC1

pSTAT3
86kDa

STAT3
85kDa

pAKT
60kDa

AKT
60kDa

IL-31 0 5 15 30 60 mins

E

HC   SSc
1 2 3 4 5 6   1 2 3 4 5 6

Collagen I
115 kDa

GAPDH
37kDa

1.DMEM only
2.DMEM + SD1029
3.IL-31 (50ng/ml)
4.IL-31 (50ng/ml) + SD1029
5.TGFβ (4ng/ml)
6.TGFβ (4ng/ml) + SD1029

F

COL1A2

2000

Relative expression

1500

1000

500

0

p<0.0045
p<0.036

Media IL-31 TGFβ   Media IL-31 TGFβ
    8 hours   24 hours

CTGF

1500

Relative expression

1000

500

0

p<0.001
p<0.001
p<0.001

Media IL-31 TGFβ   Media IL-31 TGFβ
    8 hours   24 hours

G

NF migration 6hrs

3

Scratch area mm²

2

1

0

p<0.036
p<0.0019

Media 10%FCS IL-31 IL-31+W IL-31+U

SSc migration 6hrs

3

Scratch area mm²

2

1

0

p<0.021
p<0.0067

Media 10%FCS IL-31 IL-31+W IL-31+U

NF migration 24hrs

2.0

Scratch area mm²

1.5

1.0

0.5

0.0

Media 10%FCS IL-31 IL-31+W IL-31+U

SSc migration 24hrs

1.5

Scratch area mm²

1.0

0.5

0.0

p<0.003
p<0.0001
p<0.0001
p<0.006
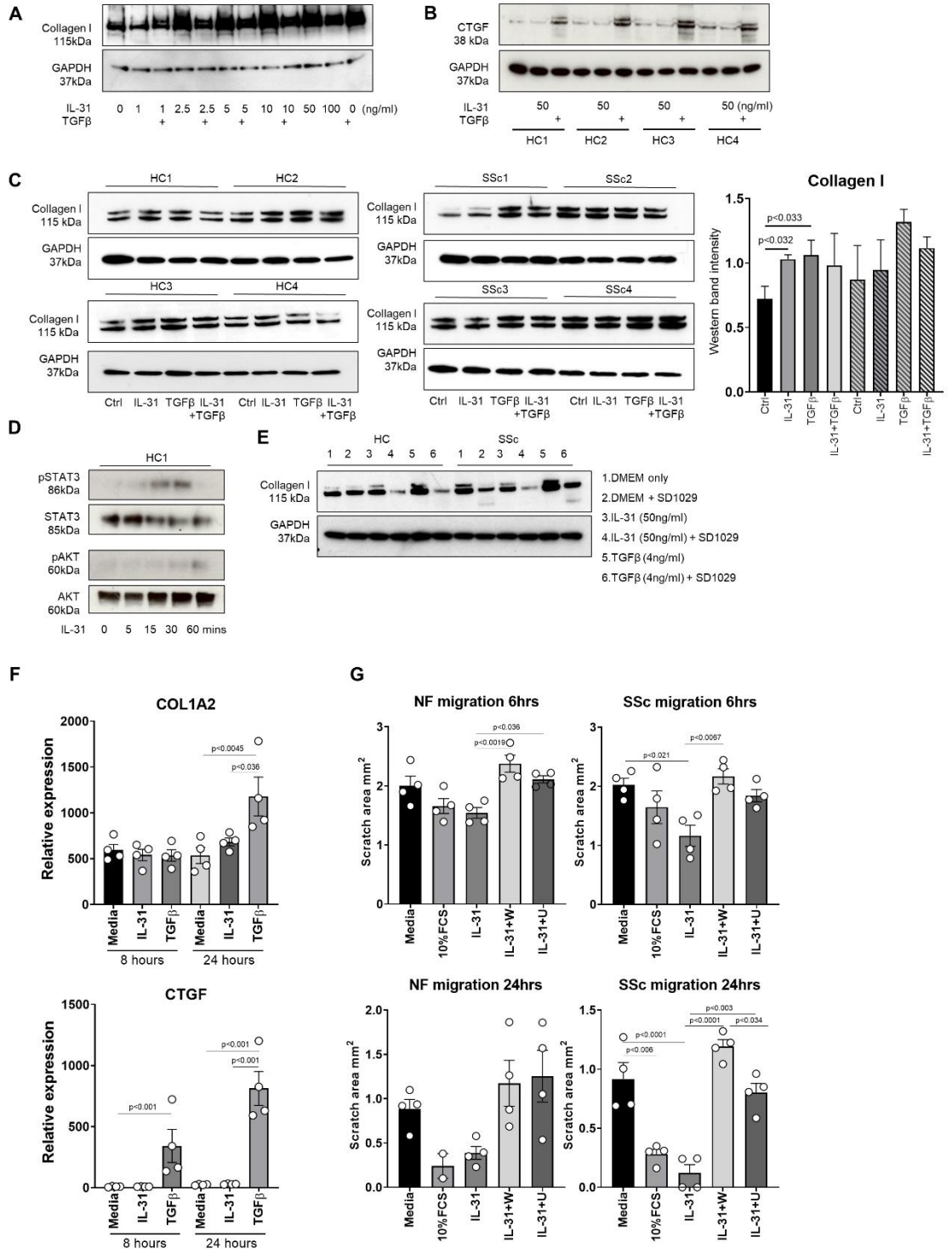p<0.034

Media 10%FCS IL-31 IL-31+W IL-31+U

Fig. 3 Phenotype changes induced in dermal fibroblasts by IL-31. Collagen I and CTGF protein levels were used to assay the fibrotic responses of human skin fibroblasts, after treatment with increasing doses of IL31 (1-100ng/ml), with or without the known pro-fibrotic TGFβ(4ng/ml). (**A**) IL-31 induced collagen I with maximal effect at 50 ng/ml (n=2 HC cell lines studied). (B) However, the matricellular protein CTGF was not induced by IL-31 (50ng/ml)(n=4 HC cell lines studied). TGFβ, as expected, induced both collagen I and CTGF protein levels, but did not appear to synergise with IL-31. (**C**) IL-31 (50 ng/ml) was used to stimulate n=4 HC and n=4 SSc dermal fibroblast lines with or without TGFβ (4ng/ml). In HC cell lines IL-31 led to a significant increase in collagen I Western band intensity (plain bars, P<0.032) as did TGFβ (p<0.033). In SSc dermal fibroblasts basal collagen I appeared higher and less responsive to IL-31 and TGFβ (hatched bars, both P NS). (**D**) IL-31 (50 ng/ml) induced signaling in normal dermal fibroblasts, causing transient phosphorylation of STAT3 and increased phosphorylation of Akt (n=2 HC fibroblast lines studied). (**E**) The STAT3 inhibitor, SD1029, substantially decreased the production of collagen I in healthy and SSc dermal fibroblasts treated with IL-31 or TGFβ(n=1 cell line for both). (**F**) IL-31 did not alter collagen I or CTGF mRNA levels in HC fibroblasts (n=4 cell lines) unlike TGFβ, indicating post-transcriptional induction of collagen I by IL-31. (**G**) IL-31 strongly enhanced migration of control and SSc dermal fibroblasts (both n=4 cell lines) at 24 hours, inhibited by Wortmannin (PI3K inhibitor, 100nM) or U0126 (MEK/ERK inhibitor, 5μM).
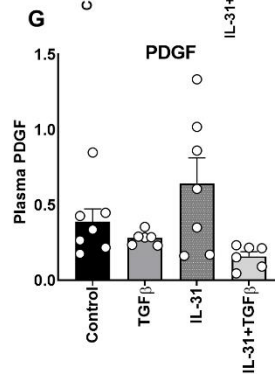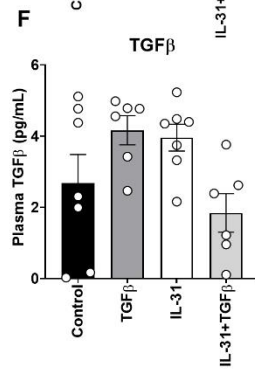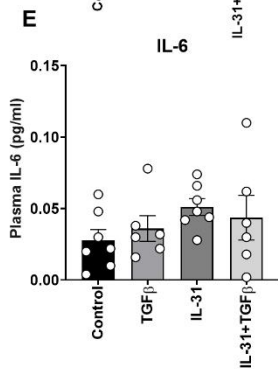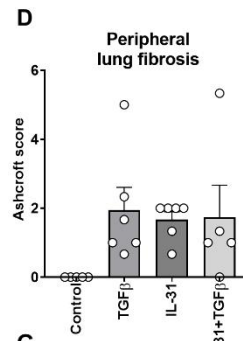
A

| | Saline | TGFβ | IL-31 | IL-31+TGFβ |

Skin H&E day 21

Skin PSR day 21

Skin Polarise day 21

Lung day 42

B Dermal collagen

PSR stain

p<0.025

Control, TGFβ, IL-31, IL-31+TGFβ

C Central lung fibrosis

Ashcroft score

p<0.033
p<0.017

Control, TGFβ, IL-31, IL-31+TGFβ

D Peripheral lung fibrosis

Ashcroft score

Control, TGFβ, IL-31, IL-31+TGFβ

E IL-6

Plasma IL-6 (pg/ml)

Control, TGFβ, IL-31, IL-31+TGFβ

F TGFβ

Plasma TGFβ (pg/mL)

Control, TGFβ, IL-31, IL-31+TGFβ

G PDGF

Plasma PDGF
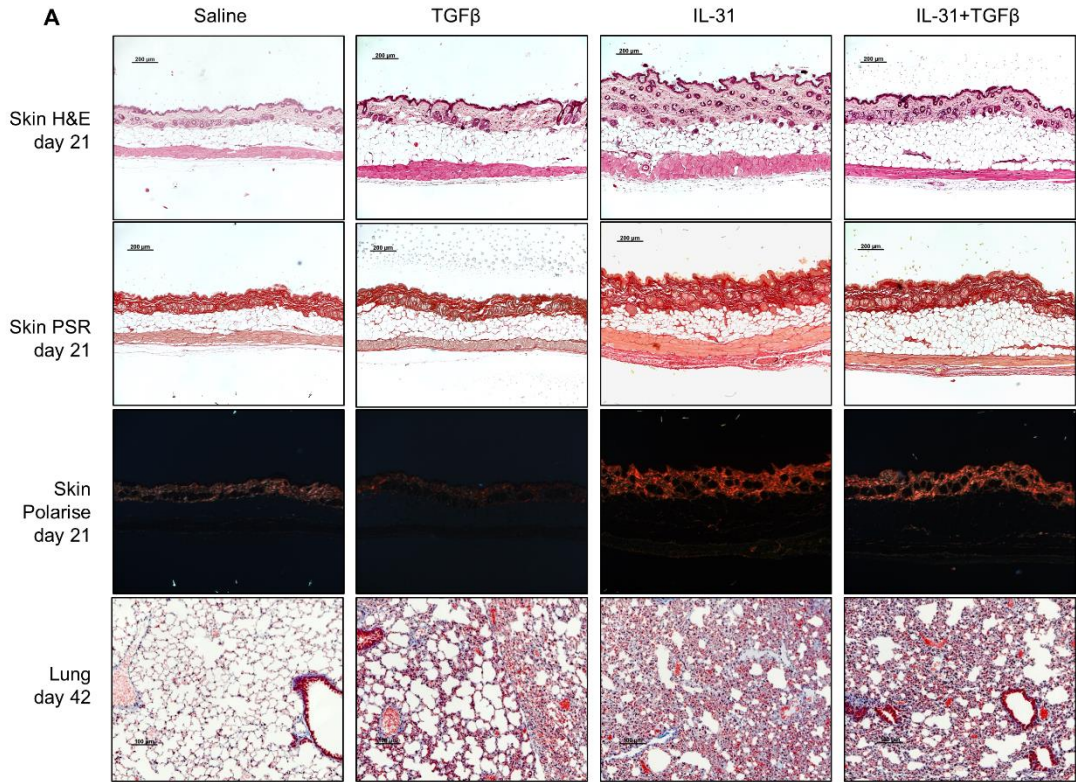
Control, TGFβ, IL-31, IL-31+TGFβ

Fig 4. IL-31 induces dermal and lung fibrosis in mice. (**A**) Wild type Balb/c mice were treated as follows: saline control (n=7 mice), TGFβ (800ng per day)(n=7), IL-31(200ng per day)(n=6) or IL-31 plus TGFβ(n=7). Each treatment was delivered continuously by an implanted subcutaneous mini pump, which was removed at day 14. At day 21 skin sections were stained for H&E or picrosirius red (PSR), revealing enhanced dermal thickening by IL-31 treatment. (**B**) Collagen cross-linking, as assessed by polarised images of PSR stain, was also enhanced by IL-31 treatment, which reached statistical significance. TGFβ alone did not cause significant increase in dermal thickness or cross-linked collagen and did not synergise with IL-31. (**C**) In further experiments using n=5-6 mice per treatment group, lung tissue sampled at day 42, demonstrated interstitial lung disease in mice treated with IL-31, similar to TGFβ treated mice, most marked in the central lung areas. Again, positive synergy was not seen. (**D**) Plasma cytokine and growth factor levels at day 21 indicated a trend towards elevated of IL-6, TGFβ1 and PDGF in IL-31 treated mice, consistent with an SSc-like fibrotic process. In general a trend towards negative synergy with TGFβ was seen in most experiments. P values for (B-D) were obtained using ANOVA and Tukey's multiple comparison test. P values <0.05 were considered significant. H&E, heamtoxylin & eosin; PSR, piscosirius red (PSR) staining.

References

1.   Allanore Y, Simms R, Distler O, Trojanowska M, Pope J, Denton CP, et al. Systemic sclerosis. Nature reviews Disease primers. 2015;1:15002.

2.   Nihtyanova SI, Schreiber BE, Ong VH, Rosenberg D, Moinzadeh P, Coghlan JG, et al. Prediction of pulmonary complications and long-term survival in systemic sclerosis. Arthritis & rheumatology (Hoboken, NJ). 2014;66(6):1625-35.

3.   Mayes MD, Bossini-Castillo L, Gorlova O, Martin JE, Zhou X, Chen WV, et al. Immunochip analysis identifies multiple susceptibility loci for systemic sclerosis. Am J Hum Genet. 2014;94(1):47-61.

4.   Bossini-Castillo L, Lopez-Isac E, Mayes MD, Martin J. Genetics of systemic sclerosis. Seminars in immunopathology. 2015;37(5):443-51.

5.   Lopez-Isac E, Campillo-Davo D, Bossini-Castillo L, Guerra SG, Assassi S, Simeon CP, et al. Influence of TYK2 in systemic sclerosis susceptibility: a new locus in the IL-12 pathway. Annals of the rheumatic diseases. 2016;75(8):1521-6.

6.   Fleischmajer R, Perlish JS, Reeves JR. Cellular infiltrates in scleroderma skin. Arthritis and rheumatism. 1977;20(4):975-84.

7.   Prescott RJ, Freemont AJ, Jones CJ, Hoyland J, Fielding P. Sequential dermal microvascular and perivascular changes in the development of scleroderma. The Journal of pathology. 1992;166(3):255-63.

8.   Mavalia C, Scaletti C, Romagnani P, Carossino AM, Pignone A, Emmi L, et al. Type 2 helper T-cell predominance and high CD30 expression in systemic sclerosis. The American journal of pathology. 1997;151(6):1751-8.

9.   Postlethwaite AE, Holness MA, Katai H, Raghow R. Human fibroblasts synthesize elevated levels of extracellular matrix proteins in response to interleukin 4. The Journal of clinical investigation. 1992;90(4):1479-85.

10.   Fuschiotti P, Larregina AT, Ho J, Feghali-Bostwick C, Medsger Jr. TA. Interleukin-13–producing CD8+ T cells mediate dermal fibrosis in patients with systemic sclerosis. Arthritis & Rheumatism. 2013;65(1):236-46.

11.   Pope JE, Bellamy N, Seibold JR, Baron M, Ellman M, Carette S, et al. A randomized, controlled trial of methotrexate versus placebo in early diffuse scleroderma. Arthritis and rheumatism. 2001;44(6):1351-8.

12.   Tashkin DP, Roth MD, Clements PJ, Furst DE, Khanna D, Kleerup EC, et al. Mycophenolate mofetil versus oral cyclophosphamide in scleroderma-related interstitial lung disease (SLS II): a

randomised controlled, double-blind, parallel group trial. The Lancet Respiratory medicine. 2016;4(9):708-19.

13. Sullivan KM, Goldmuntz EA, Keyes-Elstein L, McSweeney PA, Pinckney A, Welch B, et al. Myeloablative Autologous Stem-Cell Transplantation for Severe Scleroderma. N Engl J Med. 2018;378(1):35-47.

14. Dillon SR, Sprecher C, Hammond A, Bilsborough J, Rosenfeld-Franklin M, Presnell SR, et al. Interleukin 31, a cytokine produced by activated T cells, induces dermatitis in mice. Nature immunology. 2004;5(7):752-60.

15. Zhang Q, Putheti P, Zhou Q, Liu Q, Gao W. Structures and biological functions of IL-31 and IL-31 receptors. Cytokine Growth Factor Rev. 2008;19(5-6):347-56.

16. Nattkemper LA, Martinez-Escala ME, Gelman AB, Singer EM, Rook AH, Guitart J, et al. Cutaneous T-cell Lymphoma and Pruritus: The Expression of IL-31 and its Receptors in the Skin. Acta dermato-venereologica. 2016;96(7):894-8.

17. Kim S, Kim HJ, Yang HS, Kim E, Huh IS, Yang JM. IL-31 Serum Protein and Tissue mRNA Levels in Patients with Atopic Dermatitis. Ann Dermatol. 2011;23(4):468-73.

18. Egeberg A, Thyssen JP, Wu JJ. Anti-Interleukin-31 Receptor A Antibody for Atopic Dermatitis. N Engl J Med. 2017;376(21):2092-3.

19. Ip WK, Wong CK, Li ML, Li PW, Cheung PF, Lam CW. Interleukin-31 induces cytokine and chemokine production from human bronchial epithelial cells through activation of mitogen-activated protein kinase signalling pathways: implications for the allergic response. Immunology. 2007;122(4):532-41.

20. Wong CK, Leung KM, Qiu HN, Chow JY, Choi AO, Lam CW. Activation of eosinophils interacting with dermal fibroblasts by pruritogenic cytokine IL-31 and alarmin IL-33: implications in atopic dermatitis. PLoS One. 2012;7(1):e29815.

21. Singh B, Jegga AG, Shanmukhappa KS, Edukulla R, Khurana Hershey GH, Medvedovic M, et al. IL-31-Driven Skin Remodeling Involves Epidermal Cell Proliferation and Thickening That Lead to Impaired Skin-Barrier Function. PLoS One. 2016;11(8):e0161877.

22. Théréné C, Brenaut E, Sonbol H, Pasquier E, Saraux A, Devauchelle V, et al. Itch and systemic sclerosis: frequency, clinical characteristics and consequences. British Journal of Dermatology. 2017;176(5):1392-3.

23. Racine M, Hudson M, Baron M, Nielson WR. The Impact of Pain and Itch on Functioning and Health-Related Quality of Life in Systemic Sclerosis: An Exploratory Study. Journal of pain and symptom management. 2016;52(1):43-53.

24. van den Hoogen F, Khanna D, Fransen J, Johnson SR, Baron M, Tyndall A, et al. 2013 classification criteria for systemic sclerosis: an American College of Rheumatology/European League against Rheumatism collaborative initiative. Arthritis and rheumatism. 2013;65(11):2737-47.

25. Stratton R, Shiwen X, Martini G, Holmes A, Leask A, Haberberger T, et al. Iloprost suppresses connective tissue growth factor production in fibroblasts and in the skin of scleroderma patients. The Journal of clinical investigation. 2001;108(2):241-50.

26. Donovan J, Shiwen X, Norman J, Abraham D. Platelet-derived growth factor alpha and beta receptors have overlapping functional activities towards fibroblasts. Fibrogenesis Tissue Repair. 2013;6(1):10.

27. Hubner RH, Gitter W, El Mokhtari NE, Mathiak M, Both M, Bolte H, et al. Standardized quantification of pulmonary fibrosis in histological samples. Biotechniques. 2008;44(4):507-11, 14-7.

28. Singer EM, Shin DB, Nattkemper LA, Benoit BM, Klein RS, Didigu CA, et al. IL-31 is produced by the malignant T-cell population in cutaneous T-Cell lymphoma and correlates with CTCL pruritus. The Journal of investigative dermatology. 2013;133(12):2783-5.

29. Huang HT, Chen JM, Guo J, Lan Y, Wei YS. The association of interleukin-31 polymorphisms with interleukin-31 serum levels and risk of systemic lupus erythematosus. Rheumatol Int. 2016;36(6):799-805.

30. Kim HJ, Zeidi M, Bonciani D, Pena SM, Tiao J, Sahu S, et al. Itch in dermatomyositis: the role of increased skin interleukin-31. Br J Dermatol. 2018;179(3):669-78.

31.   Milano A, Pendergrass SA, Sargent JL, George LK, McCalmont TH, Connolly MK, et al. Molecular subsets in the gene expression signatures of scleroderma skin. PLoS One. 2008;3(7):e2696.

32.   Chakraborty D, Sumova B, Mallano T, Chen CW, Distler A, Bergmann C, et al. Activation of STAT3 integrates common profibrotic pathways to promote fibroblast activation and tissue fibrosis. Nat Commun. 2017;8(1):1130.

33.   Distler O, Highland KB, Gahlemann M, Azuma A, Fischer A, Mayes MD, et al. Nintedanib for Systemic Sclerosis-Associated Interstitial Lung Disease. N Engl J Med. 2019;380(26):2518-28.